NanoNEXT

Research Article

DOI: 10.54392/nnxt2442

Comparative Investigation of Structural, Optical and Morphological properties of Manganese Oxide and its composite

Shriya Tripathi [a,*], Narendra Kumar Pandey [a], Vernica Verma [a]

[a] Sensors and Materials Lab, Department of Physics, University of Lucknow, Lucknow, U.P.-226007, India
* Corresponding author Email: shriya97tripathi@gmail.com
DOI: https://doi.org/10.54392/nnxt2442
Received: 13-08-2024; Revised: 18-11-2024; Accepted: 01-12-2024; Published: 09-12-2024

Abstract: This work reports the successful hydrothermal synthesis of pristine β-MnO_2 and its nanocomposite with TiO_2 via solid state method. The structural analysis of the synthesised samples via X-ray diffraction spectroscopy (XRD) revealed the tetragonal phase of β-MnO_2 and β-MnO_2-TiO_2 and their high crystalline nature. The crystallinity of the pristine and composite is 71.32% and 89.17% respectively, which shows the increment in the crystallinity with the composite. The percentage of tetragonal phase of β-MnO_2 in the composite is 68.75% and the percentage of tetragonal phase of TiO_2 is 31.24%. The average crystallite size showed a decrease from 26.57nm in pristine to 22.43nm as reported in composite. The lattice strain is obtained via the W-H analysis of the samples. The lattice strain is 1.88×10^{-3} and 7.04×10^{-4} in pristine and composite shows the strain decreases in the composite. The morphology reports short nano-threads of β-MnO_2 arranged in scattered coral type structure. The composite shows dispersed granules of TiO_2 with small β-MnO_2 threads accompanied with high surface area and porosity. The UV-Visible analysis revealed the absorption peak and the optical energy band gap analysis revealed the band gap of β-MnO_2 and β-MnO_2-TiO_2. The band gap reduced to 3.6eV in composite from 4.9eV in pristine. The functional band analysis using FT-IR showed the existence of only Mn-O and both Mn-O and Ti-O vibration band in spectra of pristine and composite respectively. The increase in crystallinity, porosity and decrease in the crystallite size, strain, band gap in the nanocomposite can enhance the gas sensing application of the fabricated thin films.

Keywords: Manganese oxide, Nanocomposite, Gas Sensing Application, Thin Films, FT-IR, XRD

1. Introduction

The advent of nanoscience has revolutionized the scientific world. The nanomaterials have found several applications in various fields including medicines, sensors, electronic devices etc. This is due to the fact that the properties of the materials modify and enhance at nanoscale. The synthesis technique, average crystallite size, morphology, polymorphism etc affect the properties of the nanoparticles and hence its applications [1]. The sensing devices are a global requirement with increasing pollution and life-threatening situation arising due to gas leakage. The sensing capability of the material increases with the formation of several localized heterojunctions. The nanocomposite consists of such heterojunctions. These heterojunctions provide for a better modulation of the depletion layers. This enables the sensing device to work at lower temperatures and also increases the selectivity of the material. Manganese oxide has an oxidation state of +4. Based on the linkage of the basic octahedral units [MnO_6], the MnO_2 exists in different phases viz. α-MnO_2, β-MnO_2, γ-MnO_2 and δ-MnO_2 [2, 3]. MnO_2 has found its applications as supercapacitors, catalysts, sensors, electrode material etc. This study reports the comparative analysis of the structural, morphological and optical properties of the pristine and composite sample. The nanocomposite reported can be a promising gas sensing nanomaterial, better than the pristine material, and hence can be employed as a sensing device.

2. Materials and method

2.1. Chemicals required

The reagents used are manganese nitrate [$Mn(NO_3)_2$], potassium permanganate [$KMnO_4$], sodium hydroxide [NaOH], titanium dioxide [TiO_2], distilled water and ethanol. All the materials were of analytical grade obtained from Loba Chemie and used without any further purification.

2.2. Synthesis of β-MnO_2 and β-MnO_2-TiO_2 nanoparticles

The hydrothermal technique is used for the synthesis of sample m2 [4]. Firstly, 1.5M solution of manganese nitrate and 1M solution of potassium permanganate are separately prepared in 20 ml of distilled water. After stirring each solution separately of one hour at room temperature, the potassium permanganate solution is poured in the manganese acetate solution under continuous stirring. 2M of sodium hydroxide solution is poured into the above solution and this mixture is transferred into 100ml of Teflon lined stainless steel autoclave and placed in an oven at a temperature of 180ºC for 22 hours followed by cooling down to room temperature. The product obtained is filtered and washed with ethanol and distilled water several times and then it is placed in an oven at 80ºC for 12 hours. The dried sample is finally placed in a muffle furnace to anneal at 400ºC for 4 hours. The final pristine β-MnO_2 nanopowder sample is named m2. The solid state method is used to obtain the nanocomposite. The nanopowders of m2 and TiO_2 in the ratio of 1:1 by weight are mixed for 4 hours using the agate mortar and pestle followed by annealing the mixture at 400ºC for 2 hours. The β-MnO_2-TiO_2 nanocomposite obtained is named m4.

3. Results and Discussion

3.1. Structural Analysis

X-ray diffraction (XRD) spectroscopy provides detailed information on the phase and purity of the nanomaterial, its lattice constant, the average size of the particles of the nanomaterial. Within the 2θ range of 25^0 to 60^0 with 4^0/min scanning rate. The wavelength of the X-ray radiation used is 1.5406Å. The intensity peaks for pure MnO_2 (β-phase), are obtained at the 2θ values of 28.6^0, 37.3^0, 41.0^0, 42.7^0, 56.6^0, 59.3^0. The indices corresponding to planes associated with these peaks are given as (110), (101), (200), (111), (211) and (220) respectively. Similarly, the intensity peaks for pure TiO_2 (Anatase phase) are obtained at the 2θ values of 25.5^0, 37.1^0, 37.9^0, 38.7^0, 48.2^0, 54.0^0, 55.2^0. These peaks correspond to the planes having indices given by (101), (103), (004), (112), (200), (105) and (211) respectively. The intensity peaks of the as-synthesized nanocomposite, β-MnO_2-TiO_2, constituting both MnO_2 and TiO_2 are obtained at the 2θ values of 25.4^0, 28.7^0, 37.3^0, 38.7^0, 41.1^0, 42.7^0, 48.18^0, 54.1^0, 55.4^0, 56.7^0, 59.2^0. The corresponding indices of the diffraction planes associated with the peaks are respectively given as (101), (110), (101), (112), (200), (111), (200), (105), (211), (211) and (220). The position of the peaks stated and their relative intensities in the nanocomposite agree with the pure β-MnO_2 JCPDS card no. 24-0735 hence confirming the formation of tetragonal MnO_2 ($P4_2/mnm$ space group) [5] and, with pure TiO2 JCPDS card no. 00-021-1272 proving the formation of tetragonal TiO_2 (Anatase, I41/amd space group) [6]. For the sample m4, the calculated lattice constants are a=b=3.765Å, c= 9.487 Å and the volume is 134.48$Å^3$ for β-MnO_2 phase and a=b=4.412Å, c=2.873Å and the volume is 55.92$Å^3$ for TiO_2 phase. The lattice constants and the volume of the tetragonal structure is obtained using the respective relations $\frac{1}{d^2} = \frac{h^2+k^2}{a^2} + \frac{l^2}{c^2}$ and V=a2c [7]. The average crystallite size D is obtained using the Debye Scherrer formula given by $D = \frac{k\lambda}{\beta cos\theta}$, where, k is the Scherrer's constant or the shape factor given by k=0.91, λ is the wavelength of the incident X-ray radiation given by λ=0.15406nm, β (radians) is the full width at half maximum, θ (radians) is the Bragg's angle. The average crystallite size of m2 and m4 are 26.57nm and 22.43nm respectively. The crystallite size decreases in the composite.

The dislocation density calculated using relation $\delta=\frac{1}{D^2}$ for sample m2 and m4 are $1.41 \times 10^{-3}(nm)^{-2}$ and $1.98 \times 10^{-3}(nm)^{-2}$ respectively. Further, the crystallinity increases from 71.32% in m2 to 89.17% in m4. The composite constitutes 68.75% of tetragonal β-MnO_2 phase and 31.24% of tetragonal TiO_2 phase (anatase). Additionally, the Williamson-Hall (W-H) analysis is also employed to obtain the lattice strain induced in the sample and also their crystallite size. The slope of the W-H plot gives the lattice strain and the y-intercept is used to obtain the crystallite size. The respective lattice strain is 1.88×10^{-3} and 7.04×10^{-4} in m2 and m4, which shows the strain decreases in the nanocomposite. The strain decreases because the crystallite size decreases. The XRD pattern and Williamson-Hall plots for both pristine and nanocomposite is shown in figure 1.

3.2. Optical analysis

The method employed for the analysis of the optical properties of the synthesized samples are UV-Visible and FT-IR. The UV-Visible absorption spectrum obtained for wavelength range 190nm-800nm is depicted in the figure 2.

The plot shows the absorption band from 190nm to 240nm for m2 and from 190nm to 330nm for m4. The Tau's plot obtained using the relation $(\alpha h\upsilon) = A(h\upsilon - E_g)^n$ is used to calculate the optical energy band gap of the samples [8].

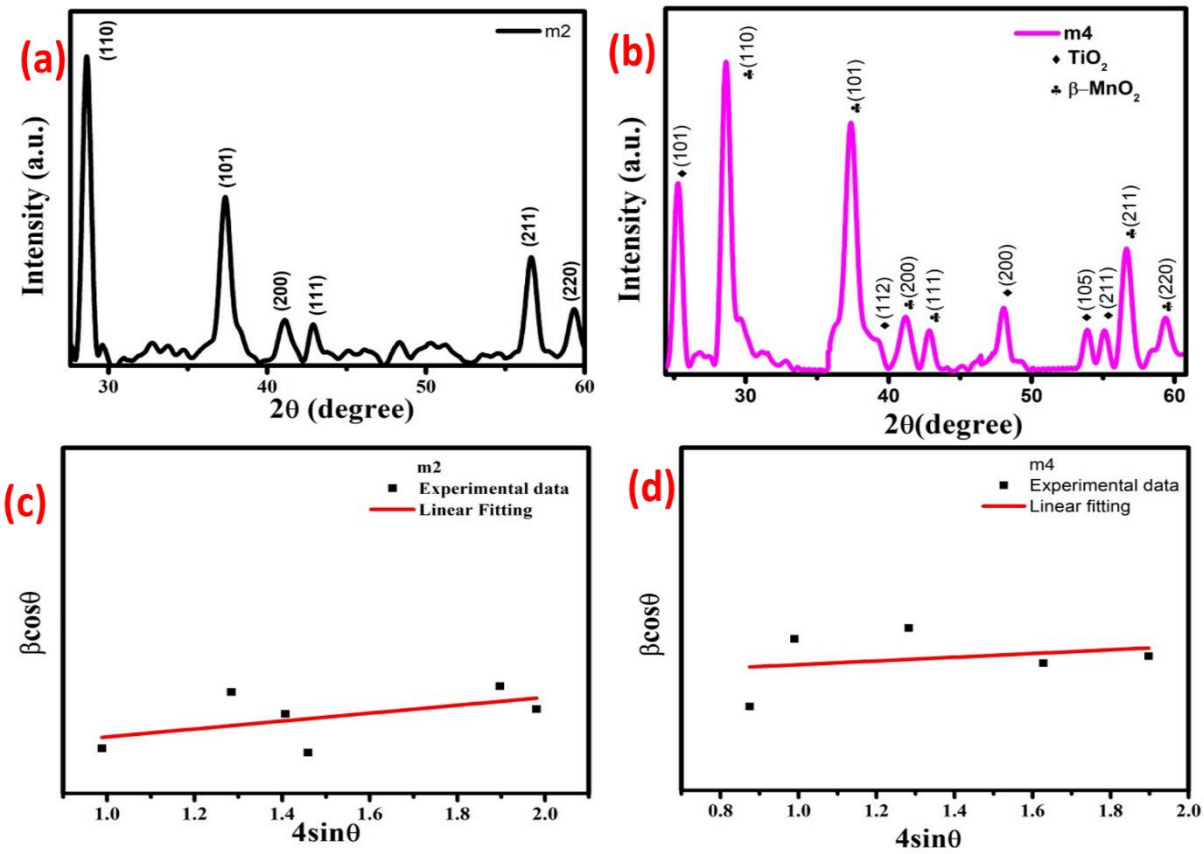

Figure 1. XRD pattern of (a) m2 (b) m4, Williamson-Hall plot for (c) m2 (d) m4.

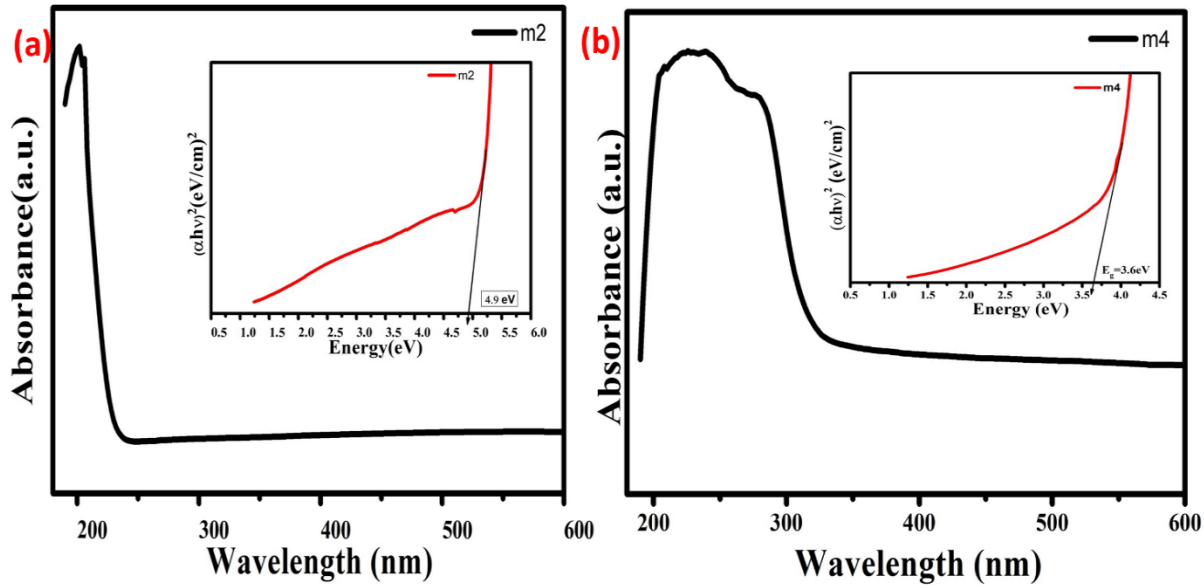

Figure 2. UV-Visible and tau plot for (a) m2 and (b) m4

A is the characteristic parameter, $h\nu$ (eV) is the photon energy, α is the absorption coefficient, E_g is the optical energy band gap, n is the characteristic of direct and indirect transition. n=1/2 and 3/2 for direct allowed and direct forbidden transition and n=2 and 3 for indirect allowed and indirect forbidden transition. Since the transition in this case is direct, therefore n=2. The band gap of m2 is 4.9eV and that of m4 is 3.6eV. This shows the decrease in the optical band gap for composite.

The FT-IR spectrum obtained for the range of 4000-400 cm^{-1} wavenumber, shown in figure 3, is used to confirm the presence of functional groups. The stretching vibrations of Mn-O occurs at 583cm^{-1} and

558 cm^{-1} whereas the stretching vibrations associated with Ti-O occurs at 678cm^{-1}. The spectrum also displays the stretching and bending -OH vibrations. This is due to the atmospheric humidity adsorbed by the samples. The C-O vibration is due to the CO_2 in the atmosphere.

3.3. Morphological Analysis

The FE-SEM technique is used to obtain the morphology of the synthesized samples. The SEM images, given in figure 4, at different magnification of the pristine sample m2 shows nano-threads and wires of variable thickness and length. The threads are so arranged that it forms a scattered coral structure. The sample m4 SEM images show the granules of TiO_2 dispersed between the short threads of β-MnO_2. Such morphology increases the surface area and porosity of the nanocomposite.

4. Conclusion

Nano-scaled sample m2 and m4 are prepared using the hydrothermal method and solid-state method respectively for comparative analysis of structural, optical and morphological properties and proposed gas sensing application of the fabricated thin films. The FE-SEM images displays their porous morphologies. X-ray diffraction patterns reveal the tetragonal structure of the nanoparticles.

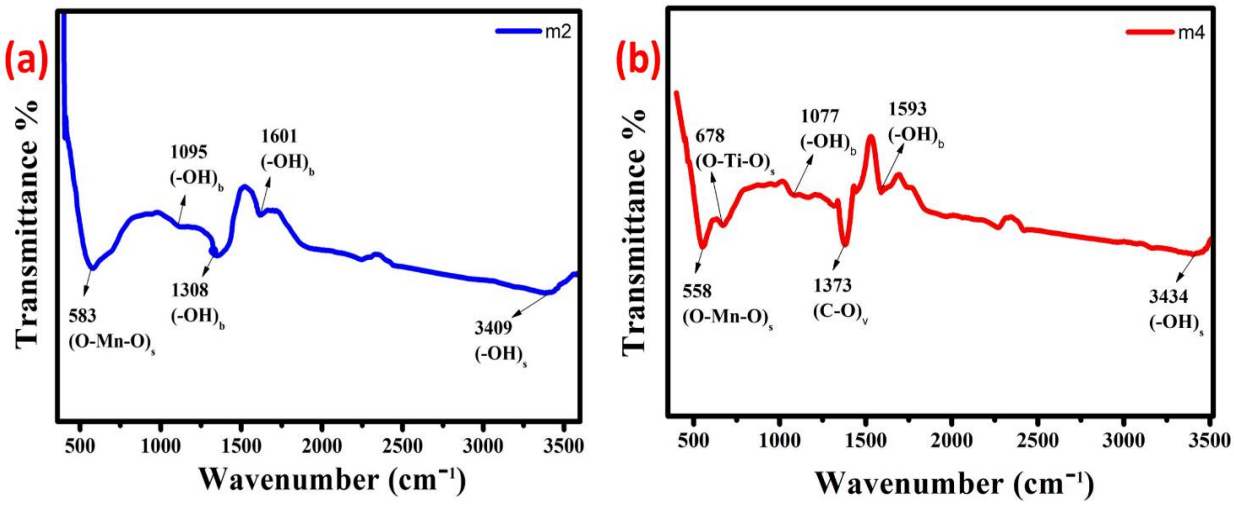

Figure 3. FT-IR spectrum for (a) m2 and (b) m4

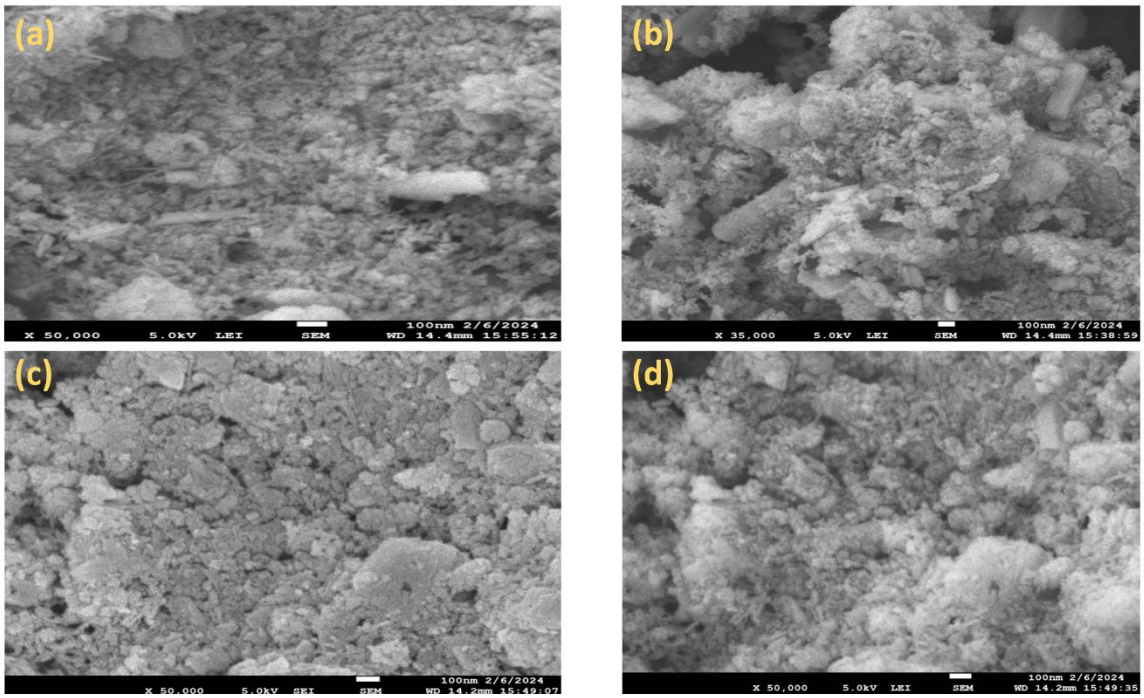

Figure 4. FE-SEM images of (a) m2 and (b) m4

The formation of nanocomposite results in decrease in crystallite size. Debye Scherrer's formula and W–H analysis are both employed to obtain the average crystallite size and the values are in good agreement with each other. The induced lattice-strain is also obtained from W-H analysis. The optical analysis shows the reduction in energy band gap. The above discussed properties of the nanocomposite can result in an efficient gas sensing device.

References

[1] X. Zhang, P. Yu, H. Zhang, D. Zhang, X. Sun, Y. Ma, Rapid hydrothermal synthesis of hierarchical nanostructures assembled from ultrathin birnessite-type MnO2 nanosheets for supercapacitor applications, Electrochimica Acta, 89, (2013) 523-529. https://doi.org/10.1016/j.electacta.2012.11.089

[2] W. Zhang, C. Zeng, M. Kong, Y. Pan, Z. Yang, Water-evaporation-induced self-assembly of a-MnO2 hierarchical hollow nanospheres and their applications in ammonia gas sensing, Sensors Actuators, B Chemical, 162(1), (2012) 292–299. https://doi.org/10.1016/j.snb.2011.12.080

[3] M.R. Sovizi, S. Mirzakhani, Highly sensitive detection of ammonia gas by 3D flower-like ϒ-MnO2 nanostructure chemiresistor, Journal of the Taiwan Institute of Chemical Engineers, 111, (2020) 293–301. https://doi.org/10.1016/j.jtice.2020.04.017

[4] B.O. Taranu, S.D. Novaconi, M. Ivanovici, J.N. Gonçalves, F.S. Rus, α-MnO2 Nanowire Structure Obtained at Low Temperature with Aspects in Environmental Remediation and Sustainable Energy Applications, Applied Sciences, 12, (2022) 6821. https://doi.org/10.3390/app12136821

[5] Z. Zhao, G. Li, Y. Sun, N. Li, Z. Zhang, J. Cheng, C. Ma, Z. Hao, The positive effect of water on acetaldehyde oxidation depended on the reaction temperature and MnO2 structure, Applied Catalysis B: Environmental, 303, (2022) 120886. https://doi.org/10.1016/j.apcatb.2021.120886

[6] B. Li, X. Wang, M. Yan, L. Li, Preparation and characterization of nano-TiO2 powder, Materials Chemistry and Physics, 78(1), (2003) 184-188. https://doi.org/10.1016/S0254-0584(02)00226-2

[7] S. Devaraj, N. Munichandraiah, Effect of crystallographic structure of MnO2 on its electrochemical capacitance properties, The Journal of Physical Chemistry C, 112, (2008) 4406-4417. https://doi.org/10.1021/jp7108785

[8] A. Verma, P. Chaudhary, A. Singh, R.K. Tripathi, B.C. Yadav, ZnS nanosheets in a polyaniline matrix as metallopolymer nanohybrids for flexible and biofriendly photodetectors, ACS Applied Nano Materials, 5, (2022) 4860-4874. https://doi.org/10.1021/acsanm.1c04437

Acknowledgement

The authors are grateful to the Department of Physics, Department of Chemistry, University of Lucknow, for providing XRD, UV-Visible and FT-IR facility for characterization.

Does this article screened for similarity?

Yes

Conflict of interest

The Authors declares that there is no conflict of interest anywhere.

About the License